Article citation info:
Zhou L, Wang W. LES of propane-air swirling non-premixed flame using a SOM combustion model. Combustion Engines. 0000;XXX(X):xx-xx. https://doi.org/10.19206/CE-197157

Lixing ZHOU
Wenli WANG

Combustion Engines
Polish Scientific Society of Combustion Engines

LES of propane-air swirling non-premixed flame using a SOM combustion model

ARTICLE INFO

Received: 1 September 2024
Revised: 11 November 2024
Accepted: 9 December 2024
Available online: 31 December 2024

Non-premixed combustion is widely encountered in engine combustors. Large-eddy simulation (LES) was used to study non-premixed combustion by previous investigators using different combustion models. In this paper, the present authors used a second-order moment (SOM) combustion model for LES of propane-air swirling non-premixed combustion for the first time. The predicted time-averaged and RMS fluctuation velocities, time-averaged temperature and species concentration are in good agreement with experimental results, showing once again the feasibility of the SOM model. The instantaneous simulation results indicate that uniform temperature distribution was observed in most regions of the combustor, probably due to the annular fuel inlet and then an expansion to the combustor. The large-eddy vortex structures intensify swirling non-premixed combustion. Swirl thickens the flame front. Unlike the jet flame, no wrinkled flame front was observed in swirling non-premixed combustion.

Key words: *swirling non-premixed propane-air flame, large-eddy simulation, second-order moment combustion model*

1. Introduction

Non-premixed swirling turbulent flames are encountered in many kinds of combustors, such as gas-turbine engine combustors, internal combustion engines and furnace burners. Syred [17] summarized the principle, application, numerical and experimental studies on swirling flows and combustion. Khaleghi et al. [8] investigated an asymmetric non-premixed meso-scale swirling flame. The flame stability, heat loss, thermal efficiency and pollutant formation were compared with each other for different air-fuel inlet velocities and chemical equivalence ratios. Furthermore, the direct photography method was used to capture flame structures in a wide range of equivalence ratios in order to emphasize exceptional flame stability. Stöhr et al. [16] and Rehm et al. [12] studied the characteristics of an oscillating rotating turbulent diffusion flame using OH-PLIF and PIV techniques. The image information of OH radical fluorescence radiation intensity in the flame was obtained by PLIF, and the flame flow field was obtained by PIV. The combustion performance and flow field characteristics of turbulent flame were shown visually. Large-eddy simulation (LES) was used to study swirling flames. Different combustion models were used. Hu et al. [3] did LES using the fast-chemistry combustion models and PIV (particle image velocimetry) measurements of methane-air non-premixed combustion, and their studies were reviewed in [25]. Both LES and PIV results showed coherent structures of flames for different fuel-air ratios, but the LES statistical results for temperature and species concentration are only in qualitative agreement with the experimental results due to neglecting the reaction kinetics in the fast-chemistry combustion model. Navarro-Martinez [11] adopted a conditional moment closure (CMC) model to simulate non-premixed combustion. Some investigators used flame-let models for LES of non-premixed flames. Xing et al. [20] used the commercial software FLUENT to select a flame-generated manifolds (FGM) approach with detailed and reduced reaction mechanisms in a large eddy simulation of a non-premixed methane-air jet flame (Sandia Flame D). Kempf et al. [7] used a flame-let model for LES of Sydney swirling non-premixed flames with different numerical methods. It was reported that the prediction results for combusting cases were not satisfactory. Zhu et al. [27] used a flame-let model in LES of non-premixed flame to study the local extinction. More complex models, like the PDF transport equation model was also used. Yang et al. [21] did a LES/PDF with an interaction-by-exchange with the mean (IEM) small-scale mixing model for non-premixed CO-H_2 jet flame and the LES results were well validated by direct numerical simulation (DNS). On the other hand, the thickened flame model was also used. Legier et al. [9] used a dynamically thickened flame model for LES of non-premixed combustion. Ke et al. [6] and Shang et al. [14] did LES of non-premixed methane-air combustion using a dynamically full thickened flame (DFTF) model and in comparison with a flame-let model. It was found that the two models gave similar results, but the DFTF can better catch the whole flame structures. Alternatively, the second-order moment (SOM) combustion model was proposed by Zhou et al. [24, 26] and was used in LES of non-premixed flames. Hu et al. [4] used the SOM combustion model for LES of swirling methane-air non-premixed flame, measured at Tsinghua University, and the Sydney swirling non-premixed flame [2]. It was found by comparison with experimental results that the SOM model is much better than the eddy-break-up (EBU) model, and swirling flames unlike the jet flame, do not have a wrinkled flame structure. Wang et al. [18] studied the Sandia methane-air jet non-premixed flame by large-eddy simulation using the SOM combustion model. Also, the SOM model gives good results. Ruihu and Teng [13] performed the LES of a methane/air co-axial jet non-premixed combustor coupled with flamelet generated manifolds (FGM) model, and the LES results were compared with experimental data. Yu et al. [22] did LES of Sandia turbulent non-premixed flame D, using both a

tabulated chemistry method coupled with three presumed probability density functions and a filtered density function (FDF)model. It was found that the latter is better. Wang et al. [19] did multi-regime mixing modeling for local extinction and re-ignition in turbulent non-premixed flame by using the LES/FDF method. Balabanov et al. [1] performed a differential subgrid stress model and its assessment in LES of non-premixed combustion. Recently Zhou et al. [24] used the SOM combustion model for LES of droplet-group combustion and found that combusting droplets reduces the drag force

It is seen that most LES of non-premixed swirling flames, including that using the SOM combustion model, were done for methane-air flames. In this paper, a large-eddy simulation is carried out for swirling propane-air non-premixed flame using the SOM combustion model for the first time. The experimental results for velocity, temperature, and species concentration assess the statistical results. The instantaneous simulation results are used to understand the flame structures.

2. Filtered govern equations for LES of turbulent flames and closure models

The filtered governing equations for LES of gas turbulent combustion can be given as [23]:

$$\frac{\partial \rho}{\partial t} + \frac{\partial}{\partial x_i}(\rho \bar{u}_i) = \bar{S} \tag{1}$$

$$\frac{\partial}{\partial t}(\rho \bar{u}_i) + \frac{\partial}{\partial x_j}(\rho \bar{u}_i \bar{u}_j) = = \frac{\partial}{\partial x_j}\left(\mu\left(\frac{\partial \bar{u}_i}{\partial x_j} + \frac{\partial \bar{u}_j}{\partial x_i}\right) - \frac{2}{3}\left(\mu \frac{\partial \bar{u}_j}{\partial x_i}\right)\delta_{ij}\right) - \frac{\partial \bar{p}}{\partial x_i} + - \frac{\partial \tau_{sgs}}{\partial x_j} + \sum_k \overline{\frac{\rho_k}{\tau_{rk}}(u_{ki} - u_i)} + \overline{u_i S} \tag{2}$$

$$\frac{\partial \rho \bar{Y}_s}{\partial t} + \frac{\partial}{\partial x_j}(\rho \bar{u}_j \bar{Y}_s) = = \frac{\partial}{\partial x_j}\left(\frac{\mu}{Sc}\frac{\partial \bar{Y}_s}{\partial x_j}\right) - \overline{w_s} - w_{sgs} - \frac{\partial g_{sgs}}{\partial x_j} + \alpha_s S \tag{3}$$

$$\frac{\partial \rho \bar{h}}{\partial t} + \frac{\partial}{\partial x_j}(\rho \bar{h} \bar{u}_j) = = \frac{\partial}{\partial x_j}\left(\frac{\mu}{Pr}\frac{\partial \bar{h}}{\partial x_j}\right) - \overline{w_s} - \frac{\partial g_{sgs}}{\partial x_j} - q_r + S_h \tag{4}$$

Here τ_{sg}, g_{sgs}, q_{sgs} and w_{sgs} denote sub-grid scale (SGS) stress, mass flux, heat flux and reaction rate respectively, needing to be closed. The SGS stress τ_{sgs} is defined by

$$\tau_{sgs} = \rho \overline{u_i u_j} - q \bar{u}_i \bar{u}_j \tag{5}$$

For the SGS stress, the Smagorinsky [15], Lilly [10] eddy-viscosity model is used as

$$\tau_{sgs} - \frac{1}{3}\tau_{kk}\delta_{ij} = -2\mu_t \overline{S_{ij}},\ \overline{S_{ij}} \equiv \frac{1}{2}\left(\frac{\partial \overline{u_i}}{\partial x_j} + \frac{\partial \overline{u_j}}{\partial x_i}\right)$$

$$\mu_t = \rho L_s^2 |\bar{S}|,\ |\bar{S}| \equiv \left(2\overline{S_{ij}S_{ij}}\right)^{1/2} \tag{6}$$

where $L_s = \min(\kappa d, C_s V^{1/3})$.The sub-grid scale mass flux and heat flux are closed by gradient modelling.

$$g_{sgs} = \rho\left(\overline{u_j Y_s} - \bar{u}_j \bar{Y}_s\right) = \frac{\mu_t}{\sigma_Y}\frac{\partial \overline{Y_s}}{\partial x_j} \tag{7}$$

$$q_{sgs} = \rho\left(\overline{u_j T} - \bar{u}_j \bar{T}\right) = \frac{\mu_t}{\sigma_T}\frac{\partial \bar{T}}{\partial x_j} \tag{8}$$

where σ_Y and σ_T are model constants, taken as $\sigma_Y = \sigma_T = = 1.0$.

The SGS reaction rate were closed using a second-order moment (SOM) combustion model, proposed by Zhou et al. [23, 26]. The instantaneous Arrhenius expression of the chemical reaction rate of a global one-step reaction is

$$w_s = B\rho^2 Y_{fu} Y_{ox} \exp\left(-\frac{E}{RT}\right) \tag{9}$$

The filtered reaction rate is

$$\overline{w_s} = \rho^2 \overline{K Y_{ox}} \overline{Y}_{fu},\ \overline{K} = B \int \exp\left(-\frac{E}{R\bar{T}}\right) p(\bar{T}) d\bar{T} \tag{10}$$

The SOM-SGS combustion model, using a gradient modeling and expressing the effect of small-scale temperature and species fluctuations on the SGS reaction rate, is given by

$$w_{sgs} = \rho^2 [\bar{K}(\overline{Y_{ox}Y_{fu}} - \bar{Y}_{ox}\bar{Y}_{fu}) + \bar{Y}_{ox}(\overline{KY_{fu}} - \bar{Y}_{fu}\bar{K}) + + \bar{Y}_{fu}(\overline{KY_{ox}} - \bar{Y}_{ox}\bar{K})] \tag{11}$$

The sub-grid scale correlation terms are given by the following algebraic expression

$$\overline{\Phi\Psi} - \bar{\Phi}\bar{\Psi} = c\mu_t \left(\frac{\partial \bar{\Phi}}{\partial x_j}\right)\left(\frac{\partial \bar{\Psi}}{\partial x_j}\right) / \rho / \left(\frac{\alpha}{\tau_T} + \frac{1-\alpha}{\tau_C}\right) \tag{12}$$

where Φ and Ψ denote Y_1 or Y_2 or K, and τ_C is the chemical reaction time, τ_T is the turbulent diffusion time, a and c are model constants, taken as a = 0.9 and c = 0.5. The reaction time and fluctuation time are given by

$$\tau_C = \left[B\rho\left(\bar{Y}_{o_2} + \beta \bar{Y}_{CH_4}\right)\exp\left(-\frac{E}{R\bar{T}}\right)\right],\ \tau_T = \frac{1}{|\bar{S}|}$$

where β is the stoichiometric coefficient.

For the propane-oxygen reaction rate, the global one-step reaction rate is adopted:

$$w_{C_3H_8} = 4.79 \cdot 10^8 \rho^{1.75} Y_{C_3H_8}^{0.1} Y_{O_2}^{0.65} \exp\left(-1.51 \cdot \frac{10^4}{T}\right) \tag{13}$$

For the radiative heat transfer, the PI model was used.

3. Simulated combustor and numerical procedure

The simulated propane-air swirling non-premixed flame was taken in a swirl combustor with an annular fuel inlet, measured in [5]. The geometrical configuration and sizes of the swirl combustor to be predicted are given in Fig. 1 and Table 1. The inlet-flow parameters are given in Table 2.

The swirl number is 0.78; the wall temperature is taken as 1373 K. The grid sizes in x, y and z directions are 1–2 mm. The total number of cells is 450,000. The grid arrangement is shown in Fig. 2. The time step is taken as 0.005 s. The convergence can be reached within each time step after 10 to 20 iterations. For the numerical procedure, the pressure-implicit split-operator (PISO) algorithm was used for p–v corrections, the second order implicit difference scheme for the time-dependent term, and the central differencing difference scheme for the convection and diffusion terms were adopted. The boundary condition

at the exit is based on a fully developed flow assumption where the gradients for all flow variables in the axial direction are zero. At the near-wall grid nodes, the wall function approximation was employed.

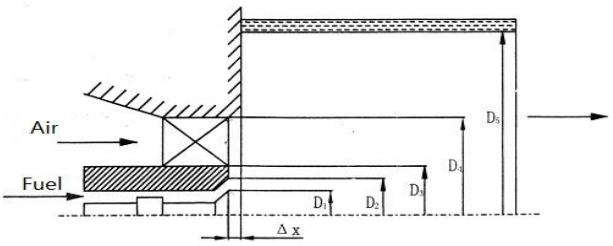

Fig. 1. A swirl combustor

Table 1. Geometrical sizes

D_1 [mm]	D_2 [mm]	D_3 [mm]	D_4 [mm]	D_5 [mm]	L [mm]
17	19	21	42	100	300

Table 2. Flow parameters

	Mass flow rate [kg/s]	Axial velocity [m/s]	Radial velocity [m/s]	Tangential velocity [m/s]	Tempe-rature [K]
Fuel inlet	$1.284 \cdot 10^{-3}$	12.43	12.43	–	294
Air inlet	$30.4 \cdot 10^{-3}$	25.96	–	25.96	313

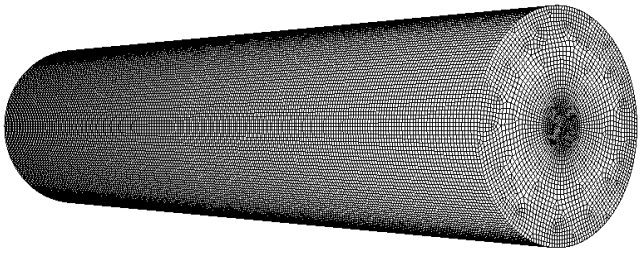

Fig. 2. Grid arrangement

4. Time-averaged simulation results and their experimental validation

The obtained time-averaged temperature, axial and tangential velocities (where u_{av} denotes the averaged inlet velocity), axial and tangential RMS fluctuation velocities, propane, CO_2 and oxygen volume fractions, validated by experimental results are shown in Fig. 3 to 10.

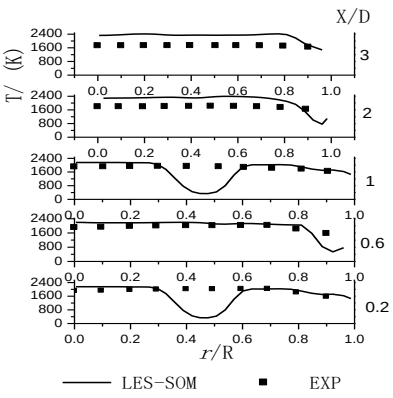

Fig. 3. Time-averaged temperature

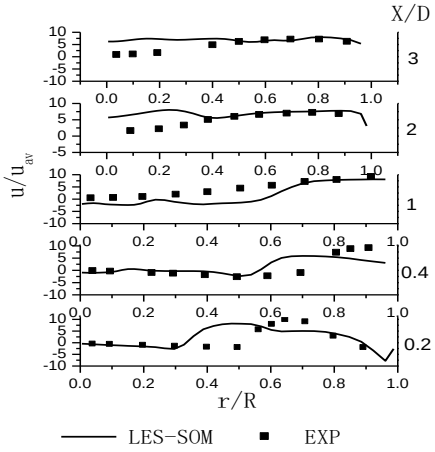

Fig. 4. Time-averaged axial velocity

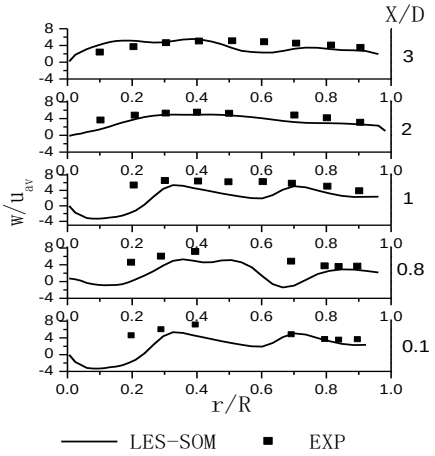

Fig. 5. Time-averaged tangential velocity

It is seen that in most regions the agreement between predictions and measurements is good. Some discrepancies between predictions and experiments are caused possibly due the assumption of uniform velocity, temperature and species concentration distributions at the inlet, but actually these distributions are non-uniform.

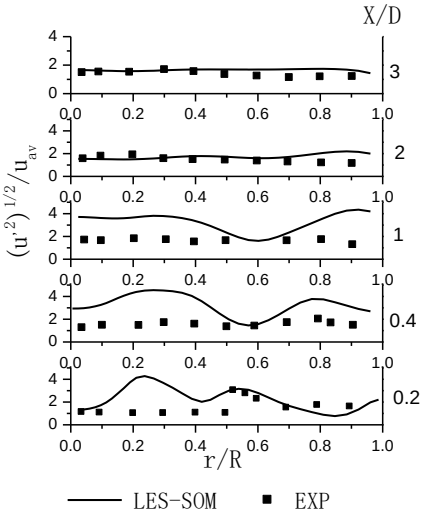

Fig. 6. Axial RMS fluctuation velocity

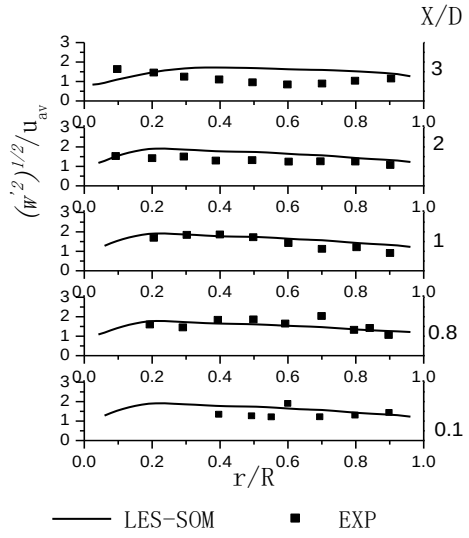

Fig. 7. Tangential RMS fluctuation velocity

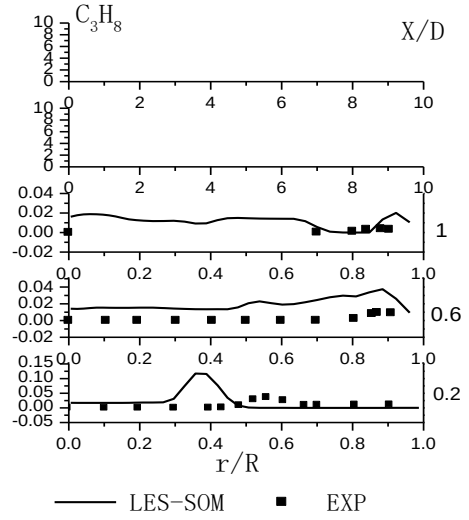

Fig. 8. Propane volume fraction

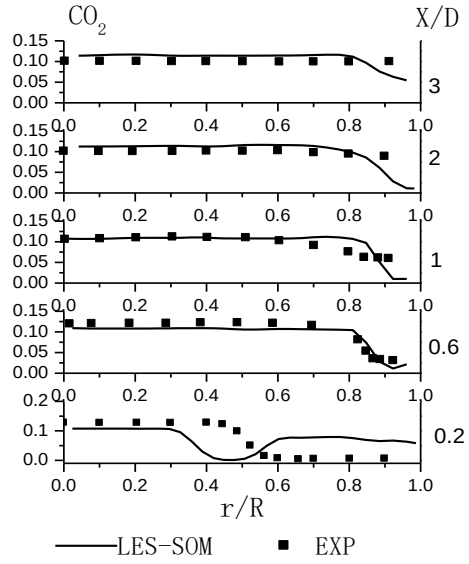

Fig. 9. CO_2 volume fraction

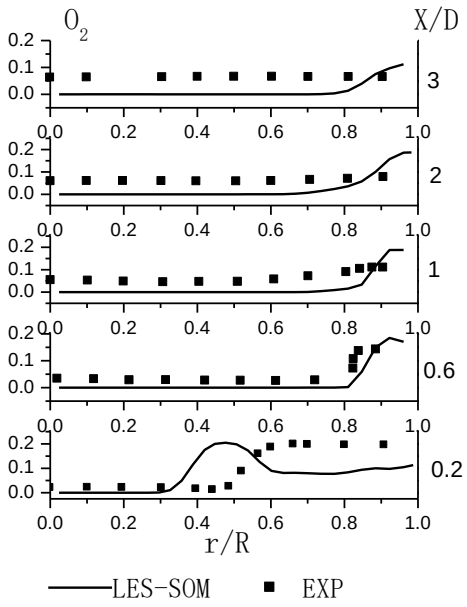

Fig. 10. Oxygen volume fraction

5. Instantaneous flame structures

Figures 11 and 12 give the instantaneous vorticity isolines in the r–z planes at $\theta = 90^0$ and $\theta = 0^0$, and in the r–θ planes at z = 40 mm, 100 mm and 250 mm respectively. The large-size vortices are at first produced near the inlet shear region and then spread to the central region. Stronger turbulence exists in these regions. The oncoming flow from the annular inlets forms a large shear layer. Many small vortices are formed around the shear layer. The shear layer diffuses quickly; the vorticity is largest near the inlet and the large vortex structures formed in the upstream region are quickly broken up.

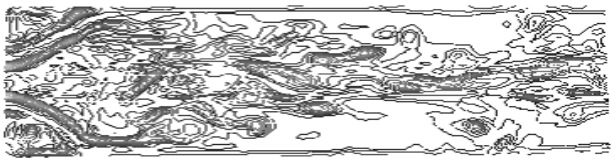

a) r–z plane, $\theta = 0^0$

b) r–z plane, $\theta = 90^0$

Fig. 11. Instantaneous vorticity isolines

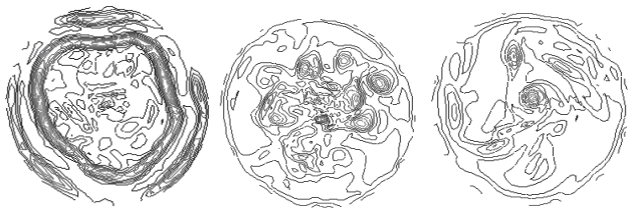

a) z = 40 mm b) z = 100 mm c) z = 250 mm

Fig. 12. Instantaneous vorticity isolines (r–θ plane)

Figures 13 and 14 show the instantaneous velocity vectors in the r–z and r–θ planes, respectively. There are two corner recirculation and many central recirculation zones, indicating the complex structure of the flow field.

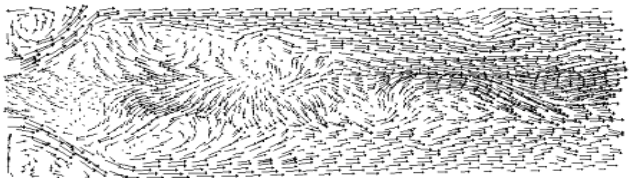

a) r–z plane, $\theta = 0^0$

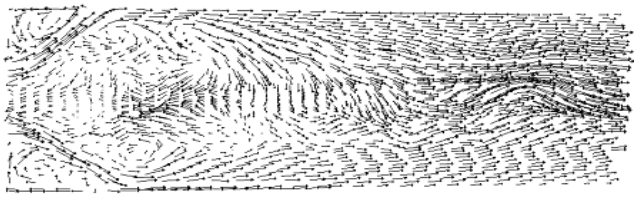

b) r–z plane, $\theta = 90^0$

Fig. 13. Instantaneous velocity vectors

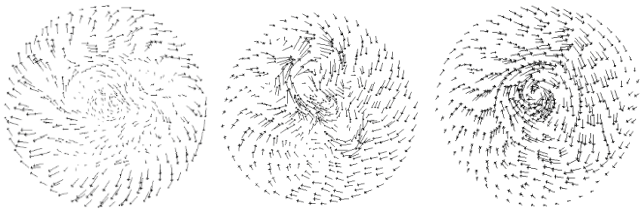

a) z = 40 mm b) z = 100 mm c) z = 250 mm

Fig. 14. Instantaneous velocity vectors (r–θ planes)

Figures 15 to 20 give obtained instantaneous temperature, propane and oxygen mass fraction maps in the r–z planes at θ = 90 and θ = 0^0, and in the r–θ plans at z = = 40 mm, 100 mm and 250 mm respectively. It is seen that the temperature distribution is rather uniform, because the fuel is supplied from an annular inlet and then discharged with an angle of expansion.

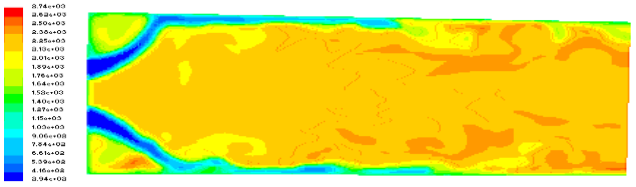

a) r–z plane, 0^0

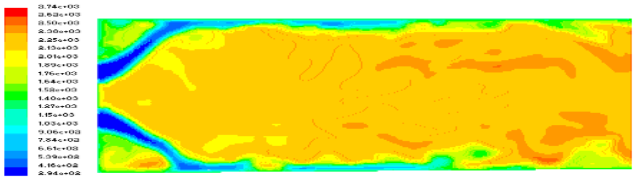

b) r–z plane, 90^0

Fig. 15. Instantaneous temperature maps

This case is different from the central supply of fuel in other swirl combustors. High temperature develops immediately behind the inlet shear region. The chemical reaction is intensified by the large-eddy structures in swirling flows. Unlike the jet flame, there is no distinct thin flame surface (wrinkled flame structure) in the swirling flame. This implies that the swirl thickens the flame front. Propane and oxygen were rapidly exhausted behind the inlet region, but some residual oxygen remains in the near-wall region, showing that combustion intensively takes place in most regions of the combustor.

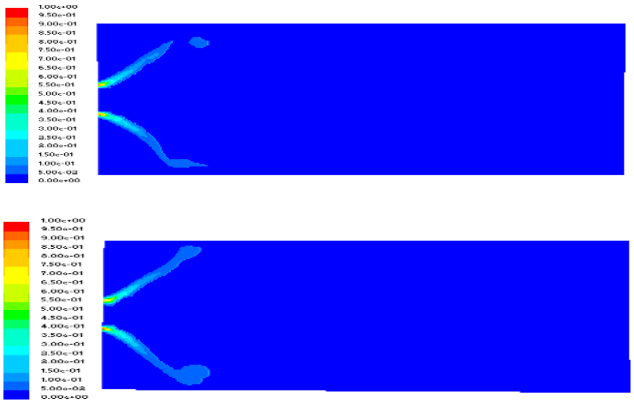

Fig. 16. Instantaneous propane mass fraction maps (top, r–z plane, 0^0) (bottom, r–z plane, 90^0)

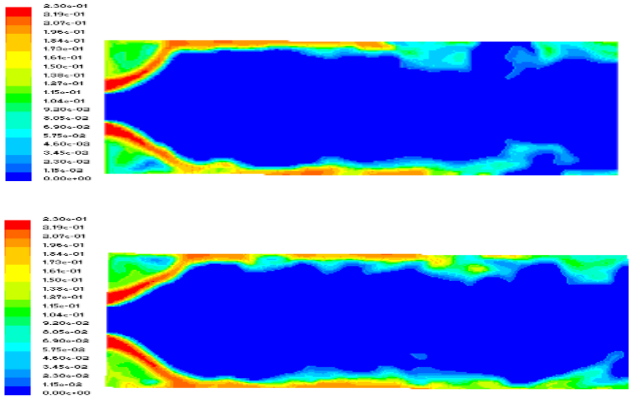

Fig. 17. Instantaneous oxygen mass fraction maps (top, r–z plane,0^0) (bottom, r–z plane, 90^0)

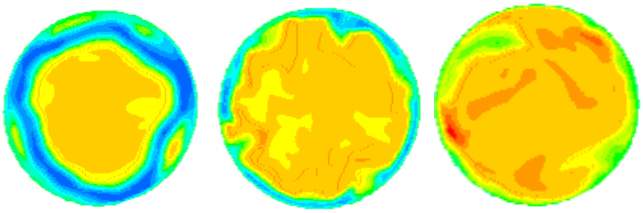

z = 40 mm z = 100 mm z = 250 mm

Fig. 18. Instantaneous temperature maps (r–θ plane)

z = 40 mm z = 100 mm z = 250 mm

Fig. 19. Instantaneous propane mass fraction maps (r–θ plane)

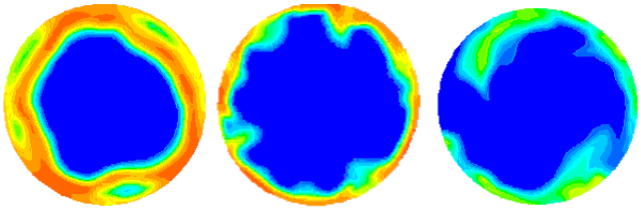

z = 40 mm z = 100 mm z = 250 mm

Fig. 20. Instantaneous oxygen mass fraction maps (r–θ plane)

Conclusions

1. The swirling propane-air non-premixed combustion was studied by large-eddy simulation using a second-order moment (SOM) combustion model. The statistical results for time-averaged temperature, species concentration, time-averaged and RMS fluctuation velocities were well validated by experimental results, indicating that the simulation results are reliable and the SOM combustion model is good for simulating complex turbulent flames.
2. A complex flow structures with many large-scale structures produced by the highly shear near the inlet were observed, where strong turbulence is located.
3. Uniform temperature distribution was observed in most regions of the combustor, probably due to the annular fuel inlet and then an expansion to the combustor.
4. The large-eddy vortex structures intensify swirling non-premixed combustion. Swirl thickens the flame front.
5. Unlike the jet flame, no wrinkled flame front was observed in swirling non-premixed combustion.
6. Multiple and detailed reaction mechanisms are needed instead of the one-step global reaction mechanism in the SOM combustion model.

Acknowledgements

This study was sponsored by the Project of National Natural Science Foundation of China under the Grant 51390493.

Bibliography

[1] Balabanov R, Usov L, Troshin A, Vlasenko V, Sabelnikov V. A differential subgrid stress model and its assessment in large eddy simulations of non-premixed turbulent combustion. Appl Sci. 2022;12(17):8491. https://doi.org/10.3390/app12178491

[2] Hu LY, Zhou LX, Luo YH. Large-eddy simulation of the sydney swirling nonpremixed flame and validation of several subgrid-scale models. Numer Heat Tr B-Fund. 2008;53(1):39-58. https://doi.org/10.1080/10407790701632477

[3] Hu LY, Zhou LX, Luo YH, Xu CS. Experimental validation of Large-eddy simulation for swirling methane-air non-premixed combustion. Qi H, Zhao B (ed.). Cleaner Combustion and Sustainable World. Berlin, Heidelberg: Springer Berlin Heidelberg; 2013. 201-207. https://doi.org/10.1007/978-3-642-30445-3_31

[4] Hu LY, Zhou LX, Zhang J. Large-eddy simulation of a swirling diffusion flame using a SOM SGS combustion model. Numer Heat Tr B-Fund. 2006;50(1):41-58. https://doi.org/10.1080/10407790500459395

[5] Jones WP, Wilhelmi J. Velocity, temperature and composition measurements in a confined swirl driven recirculating flow. Combust Sci Technol. 1989;63(1):13-31. https://doi.org/10.1080/00102208908947115

[6] Ke Z, Tao SM et al. Large-eddy simulation of methane/air non-premixedc ombustion using dynamically full thickened flame model. J Eng Thermophys (in Chinese), 2012;33:1823-1926,

[7] Kempf A, Malalasekera W, Ranga-Dinesh KKJ, Stein O. Large eddy simulations of swirling non-premixed flames with flamelet models: a comparison of numerical methods. Flow Turbul Combust. 2008;81(4):523-561. https://doi.org/10.1007/s10494-008-9147-1

[8] Kleghi M, Hosseini SE, Wahid MA. Investigations of asymmetric non-premixed meso-scale vortex combustion. Appl Therm Eng. 2015;81:140-153. https://doi.org/10.1016/j.applthermaleng.2015.02.022

[9] Légier JP, Poinsot T, Varoquié B, Lacas F, Veynante D. Large eddy simulation of a non-premixed turbulent burner using a dynamically thickened flame model. Pollard A, Candel S (eds). IUTAM Symposium on Turbulent Mixing and Combustion. Springer Netherlands; 2002. 315-326. https://doi.org/10.1007/978-94-017-1998-8_27

[10] Lilly D. On the application of the eddy viscosity concept in the Inertial sub-range of turbulence. UCAR/NCAR 1966, 675. https://doi.org/10.5065/D67H1GGQ

[11] Navarro-Martinez S. Conditional moment closure methods for turbulent non-premixed combustion. In: De S, Agarwal AK, Chaudhuri S, Sen S (ed.). Modeling and simulation of turbulent combustion. Springer Singapore; 2018. 291-310. https://doi.org/10.1007/978-981-10-7410-3_9

[12] Rehm J, Clemens N, Rehm J, Clemens N. A PIV/PLIF investigation of turbulent planar non-premixed flames. 35th Aerospace Sciences Meeting and Exhibit. Reno: American Institute of Aeronautics and Astronautics, 2013. https://doi.org/10.2514/6.1997-250

[13] Ruihu F, Teng Z. Large eddy simulation of co-axial jet non-premixed combustion using FGM model. Journal of Engineering for Thermal Energy and Power (in Chinese). 2023;38(5):42-49. https://doi.org/10.16146/j.cnki.rndlgc.2023.05.005

[14] Shang M-T, Zhang W-P, Zhang K, Fan RJ. Three-dimensional full compressible large-eddy simulation of non-premixed combustion using dynamically thickened flame model. Journal of Combustion Science and Technology (in Chinese). 2010;16:496-502.

[15] Smagorinsky J. General circulation experiments with the primitive equations: I. the basic experiment. Mon Wea Rev. 1963;91(3):99-164. https://doi.org/10.1175/1520-0493(1963)091<0099:GCEWTP>2.3.CO;2

[16] Stöhr M, Sadanandan R, Meier W. Experimental study of unsteady flame structures of an oscillating swirl flame in a gas turbine model combustor. P Combust Inst. 2009; 32(2):2925-2932. https://doi.org/10.1016/j.proci.2008.05.086

[17] Syred N. 40 Years with swirl, vortex, cyclonic flows, and combustion. 49th AIAA Aerospace Sciences Meeting Including the New Horizons Forum and Aerospace Exposition. Orlando, Florida: American Institute of Aeronautics and Astronautics, 2011. https://doi.org/10.2514/6.2011-105

[18] Wang F, Zhou L, Xu C. Large-eddy simulation of correlation moments in turbulent combustion and validation of the RANS-SOM combustion model. Fuel. 2006;85(9):1242-1247. https://doi.org/10.1016/j.fuel.2005.11.006

[19] Wang H, Kashyap S. Multi-regime mixing modeling for local extinction and re-ignition in turbulent non-premixed flame by using LES/FDF method. Flow Turbul Combust. 2023;111(1): 211-234. https://doi.org/10.1007/s10494-023-00411-8

[20] Xing Y, Zhang T, Tian Z, Li J, Yan Y. Large eddy simulation of a turbulent non-premixed flame based on the flamelet-generated manifolds approach and a reduced mechanism verification. Aerosp Sci Technol. 2020;105:105952. https://doi.org/10.1016/j.ast.2020.105952

[21] Yang Y, Wang H, Pope SB, Chen JH. Large-eddy simulation/ probability density function modeling of a non-premixed CO/H_2 temporally evolving jet flame. P Combust Inst. 2013; 34(1):1241-1249. https://doi.org/10.1016/j.proci.2012.08.015

[22] Yu Z, Huang L, Ye T, Zhu M. Large eddy simulations of high Reynolds number turbulent non-premixed flame and NO formation. Acta Aerodynamica Sinica (in Chinese), 2020; 38:629-640. https://doi.org/10.7638/kqdlxxb-2020.0036

[23] Zhou L. Development of SOM combustion model for Reynolds-averaged and large-eddy simulation of turbulent combustion and its validation by DNS. Sci China Ser E-Technol Sci. 2008;51(8):1073-1086. https://doi.org/10.1007/s11431-008-0157-y

[24] Zhou L, Li K, Sun T. Studies on the flame structure and drag of a combusting droplet group. Combustion Engines. 2023; 193(2):3-8. https://doi.org/10.19206/CE-160506

[25] Zhou LX, Hu LY. Measurement and simulation of non-premixed flames: A selected review. Int J Model Simul Sci Comput. 2023;14(04):2350014. https://doi.org/10.1142/S1793962323500149

[26] Zhou LX, Qiao L, Chen XL, Zhang J. A USM turbulence-chemistry model for simulating NOx formation in turbulent combustion. Fuel. 2002;81(13):1703-1709. https://doi.org/10.1016/S0016-2361(01)00173-9

[27] Zhu W-Z, Yang J-Z, Chen J, Chen Y-L. Large eddy simulation of local extinction of turbulent non-premixed flame. Journal of Propulsion Technology (in Chinese), 2015; 36(6):808-815. https://doi.org/10.13675/j.cnki.tjjs.2015.06.002

Prof. Lixing Zhou, DSc., DEng. – Engineering Mechanics, Tsinghua University, China.
e-mail: *zhoulx@mail.tsinghua.edu.cn*

Wenli Wang, DEng. – Engineering Mechanics, Tsinghua University, China.
e-mail: *wangwenli@smail.tsinghua.edu.cn*